

# Noncovalent Functionalization of Multiwalled Carbon Nanotubes: Application in Hybrid Nanostructures

Tie Wang, Xiaoge Hu, Xiaohu Qu, and Shaojun Dong\*

State Key Laboratory of Electroanalytical Chemistry, Changchun Institute of Applied Chemistry, Chinese Academy of Sciences, Changchun, Jilin 130022, People's Republic of China, and Graduate School of the Chinese Academy of Sciences, Beijing, 100039, People's Republic of China

Received: December 8, 2005; In Final Form: January 23, 2006

We developed a reproducible, noncovalent strategy to functionalize multiwalled carbon nanotubes (MWNTs) via embedding nanotubes in polysiloxane shells. (3-Aminopropyl)triethoxysilane molecules adsorbed to the nanotube surfaces via hydrophobic interactions are polymerized simply by acid catalysis and form a thin polysiloxane layer. On the basis of the embedded MWNTs, negatively charged gold nanoparticles are anchored to the nanotube surfaces via electrostatic interactions between the protonated amino groups and the gold nanoparticles. Furthermore, these gold nanoparticles can further grow and magnify along the nanotubes through heating in  $\text{HAuCl}_4$  aqueous solution at 100 °C; as a result these nanoparticles are joined to form continuous gold nanowires with MWNTs acting as templates.

## Introduction

The unique electronic, physical, and chemical properties of carbon nanotubes have led researchers to explore their use in composite materials for a variety of applications, including electrostatic discharge,<sup>1</sup> ultrahigh-strength engineering fibers,<sup>2</sup> and quantum wires.<sup>3</sup> The functionalization chemistry of the open ends, the exterior walls (convex face), and the interior cavity (concave face) of the carbon nanotubes is expected to play a vital role in tailoring the properties of these materials and the engineering of nanotube devices.<sup>4</sup> However, a major barrier for developing and studying such carbon-nanotube-based devices is the poor solubility and processibility of carbon nanotubes.<sup>5</sup> Since the sidewall of carbon nanotubes is chemically stable, the noncovalent functionalization of the nanotubes sidewall still presents a challenge. In addition, the nanoparticles could be as versatile building blocks for the construction of nanodevices.<sup>6</sup> Certain functional groups decorated on the carbon nanotubes can selectively bind such nanoparticles to the nanotube surfaces. The hybrid nanostructures composed of carbon nanotubes and nanoparticles are of interest and may be used in electronic, magnetic, or catalytic applications.<sup>7</sup> Presently, various approaches for nanoparticles/carbon nanotubes hybrid nanostructures have been used. One of the most well developed approaches involves the introduction of carboxylic acid groups onto their surfaces via an acid treatment, wherein nanoparticles are attached to the carbon nanotubes by covalent, noncovalent, and electrostatic interactions.<sup>8</sup> To date, the investigation of metal/carbon nanotubes hybrid nanostructures was mainly concentrated on the self-assembly between nanoparticles and carbon nanotubes.<sup>9</sup> Many efforts to fabricate gold nanowires for which carbon nanotubes serve as template have just begun.<sup>10</sup> Such assemblies may meet the demand for future application of nanodevices, which allow the further miniaturization of integrated circuits.<sup>11</sup>

Here, we develop a noncovalent method of modifying multiwalled carbon nanotubes (MWNTs) by embedding the nanotubes within polysiloxane micelles. In addition, because the polysiloxane shell is very fixed, the functionalization of MWNTs is stabilized with respect to typical polymer processing. Another advantage in our strategy is that they can be easily defunctionalized by eroding with hydrofluoric acid, allowing the recovery of nanotubes from polysiloxane shell. We use the polysiloxane shell to selectively attach gold nanoparticles to the MWNT surfaces. These nanoparticles attached on the MWNTs can grow and magnify along the nanotubes through heating in the  $\text{HAuCl}_4$  aqueous solution at 100 °C. Prolonging the heating process, these growing nanoparticles are joined and form continuous gold nanowires along the nanotubes.

## Experimental Section

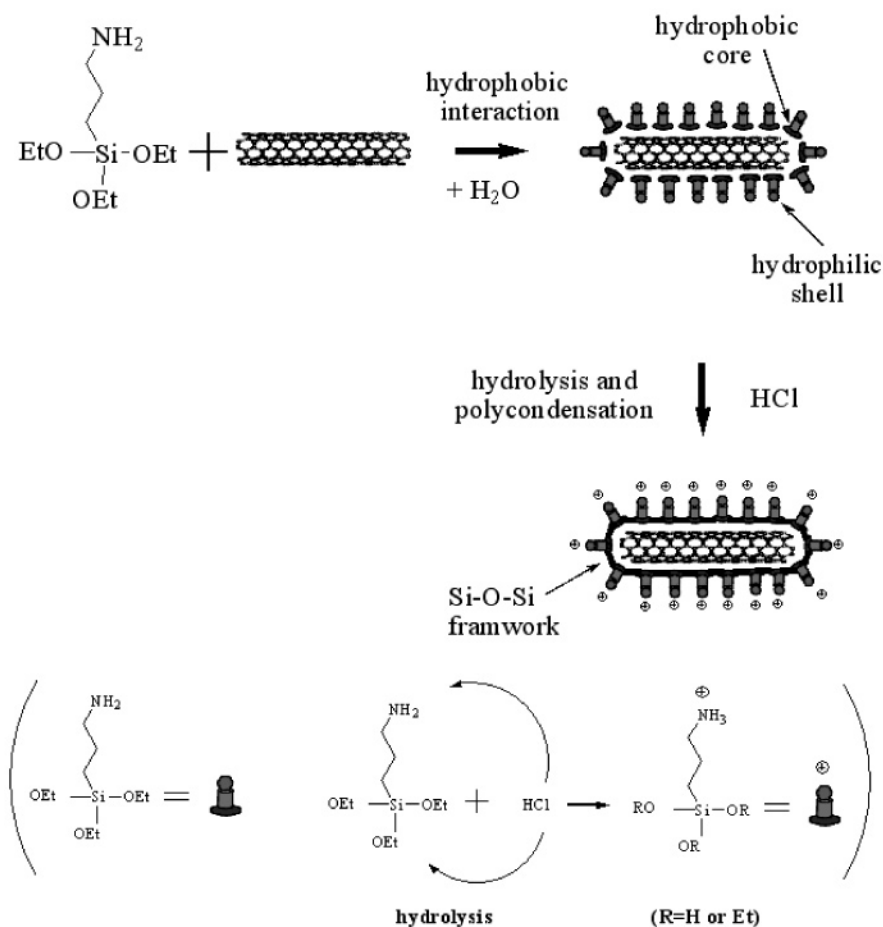
**Materials.** Hydrogen tetrachloroaurate(III) trihydrate ( $\text{HAuCl}_4 \cdot 3\text{H}_2\text{O}$ , 99.9+%), trisodium citrate dihydrate (99%), hexadecyltrimethylammonium bromide (CTAB, 98%), sodium borohydride ( $\text{NaBH}_4$ , 99%), and (3-aminopropyl)triethoxysilane (3-APTES) were all purchased from Aldrich. MWNTs were obtained from Nanotech Port Ltd. Co. (95% purity; Shenzhen, China). The MWNTs were heat-treated at 1730 °C under vacuum for 5 h, as previously reported,<sup>12</sup> washed with  $\text{CS}_2$  and toluene, and centrifuged, and the solid material was dried in a vacuum oven at 50 °C for 48 h before use.

**Instrumentation.** The gold slate coated with MWNTs was imaged by an XL30 ESEM FEG field emission scanning electron microscopy (SEM, FEI Company with 20 kV operating voltage) equipped with energy-dispersive X-ray (EDX). Transmission electron microscopy (TEM) was performed with a HITACHI H-8100 EM with accelerating voltage 200 kV. Optical spectra were acquired using a Cary 500 UV–visible NTR spectrometer (Varian). Photographs were taken by a FinePixViewer 6900 camera made by Fuji Photo Film Co., Ltd.

**Preparation of the Gold Nanoparticles.** The procedure that produced spherical gold nanoparticles 5 nm in average diameter followed the method of Murphy.<sup>13</sup> Briefly, 18.40 mL of distilled

\* Corresponding author. Tel: +86-431-5262101. Fax: +86-431-5689711. E-mail: dongsj@ciac.jl.cn.

## SCHEME 1: MWNTs Embedded in the Polysiloxane Shells



water, 0.50 mL of an aqueous 0.01 M  $\text{HAuCl}_4 \cdot 3\text{H}_2\text{O}$  solution, and 0.50 mL of an aqueous 0.01 M trisodium citrate solution were mixed. Next, 0.60 mL of 0.1 M  $\text{NaBH}_4$  aqueous solution was added in (total volume 20.00 mL) with stirring. The solution turned to pink, which indicated the formation of gold nanoparticles.

**The Embedment of MWNTs with Polysiloxane.** Typically, 5.00 mg of MWNTs were added to 2.00 mL of distilled water and could not be dispersed by ultrasonication in a laboratory ultrasonic bath (300 W and 40 kHz; Shanghai Lustration Ultrasonic Equipment Factory). After adding 0.50 mL of 3-APTES, with the help of ultrasonication for 2 min, a homogeneous, well-dispersed suspension could be easily prepared (Figure S1 of the Supporting Information). Next, the siloxane micelles were cross-linked with Si-O-Si framework by addition of 0.04 mL of hydrochloric acid (0.1 M). After the cross-linking, excess reagents were removed by dialysis of the suspension against distilled water. The polysiloxane-embedded MWNTs (Si-MWNTs) were purified from the suspension by four cycles of centrifuging the suspension and discarding the supernatant. The Si-MWNTs were dried in a vacuum oven at 50 °C for about 2 h for further use. The purified Si-MWNTs could be redispersed in distilled water at a concentration of 2.50  $\text{mg mL}^{-1}$  with ultrasonication for 2 min (Figure S2 of the Supporting Information). The dispersibility of carbon nanotubes in water can be attributed to the presence of a large numbers of amino groups on the surfaces of the carbon nanotubes.

**The Assembly and Growth of Gold Nanoparticles on Si-MWNTs.** In a typical preparation procedure, 0.50 mg of purified Si-MWNTs was dispersed in 1.00 mL of distilled water and mixed with 1.00 mL of prepared gold colloid. The system was

kept for various times (from 1 to 8 h) at ambient temperatures (around 20 °C). After centrifugation, the black solids left at bottom of the container were extensively washed with distilled water to remove free gold nanoparticles four times. The negatively charged gold nanoparticles were anchored on the surface of the nanotubes through electrostatic interaction between the amino groups and the nanoparticles. A drop of the sample redispersed in distilled water was deposited on a microgrid and dried in air for TEM characterization. Then, the as-prepared hybrid nanostructures based on Si-MWNTs decorating with gold nanoparticles (0.20 mg, self-assembled time was 1 h) were dispersed in 24.3 mM  $\text{HAuCl}_4$  aqueous solution and heated at 100 °C for 30 min in an autoclave. The continuous gold nanowires were obtained on the surfaces of Si-MWNTs.

## Results and Discussion

Our strategy for embedding MWNTs within polysiloxane shells (Scheme 1) is similar to formation of rodlike micelles with hydrolyzed siloxane.<sup>14</sup> The embedment can originate from the formation of the siloxane micelle consisting of a hydrophilic amino group site outside and an alkoxy silane site inside in an aqueous solution.<sup>14</sup> With the presence of MWNTs, the siloxane will be attached to the nanotube surfaces on the basis of hydrophobic interactions and then polymerized simply through acid catalysis. As a result, the MWNTs are permanently embedded in the polysiloxane shell with amino groups extruding outside, which are different from the previous route proposed by Liu and co-workers based on the interaction between amino groups and carbon nanotube sidewalls.<sup>5g</sup> The extruding amino groups can offer convenient ways for further functionalization of carbon nanotubes.

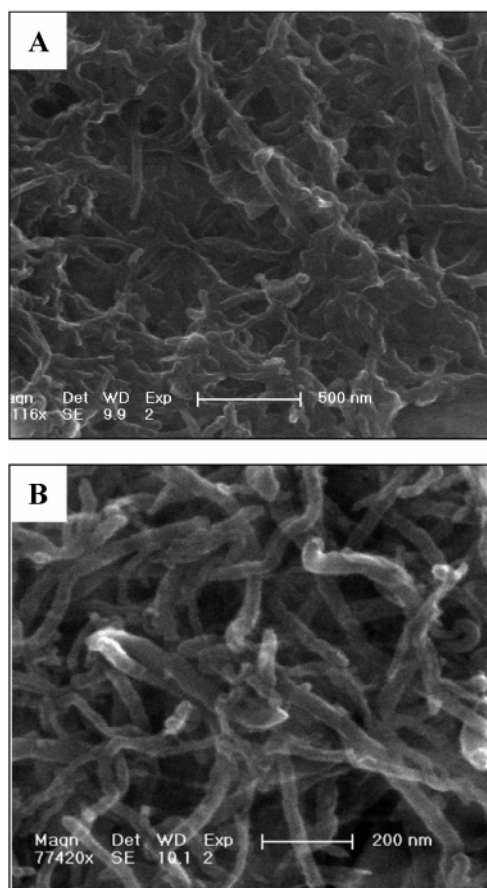


**Figure 1.** SEM images of Si-MWNT samples on the gold slates (A) before and (B) after purification.

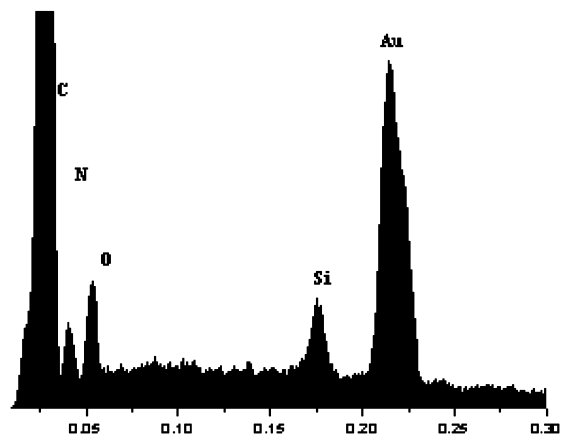


**Figure 2.** EDX spectra of purified Si-MWNTs with gold substrates.

Both the Si-MWNTs before and after separated from siloxane solution were characterized by SEM, as shown in Figure 1. When the Si-MWNTs are directly deposited on the substrate without centrifugation and washing with water, they seem to be decorated in the siloxane films and the morphology of the carbon nanotubes is not clear (Figure 1A). After centrifugation and washing, the former siloxane films disappear, showing a clear morphology of the carbon nanotubes (Figure 1B). It indicates that the excess siloxanes have been successfully removed and that the purified Si-MWNTs are obtained. Furthermore, the EDX spectrum reveals the presence of O, N, and Si with a relative ratio of 3:2:2 on the purified Si-MWNTs (Figure 2), which is consistent with the molecular structure of polymerized 3-APTES. Au and C peaks originate from gold substrate and carbon nanotubes, respectively. As a comparison,

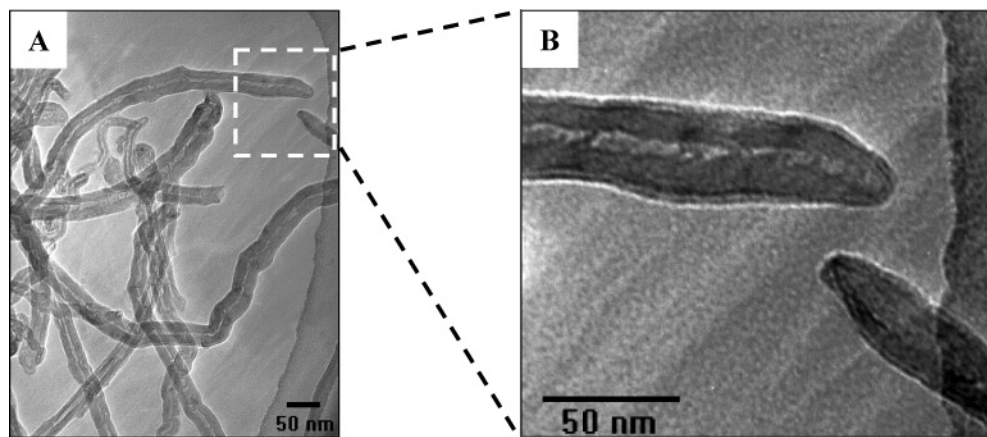
none of these elements were observed on pristine MWNTs by elemental analysis. Therefore, the peaks of Si, N, and O for Si-MWNTs can be attributed to the polymerized 3-APTES on the surface of MWNTs.

Figure 3 shows the TEM images of purified Si-MWNTs redispersed in distilled water. The general length of the Si-MWNTs ranges from a few hundred nanometers to several micrometers, and the typical diameters of Si-MWNTs are 20–45 nm. The TEM image provides the most direct evidence for the presence of polysiloxane on the nanotube surfaces (Figure 3B) and demonstrates that the siloxane contains individual MWNTs rather than MWNTs bundles. In general, the polysiloxane shell exhibits a smooth and continuous cylinder layer on the nanotube surfaces. In addition, we consider that MWNTs are embedded in multilayers, rather than monolayer polysiloxane shells. When a monolayer of 3-APTES is absorbed on the surface of MWNTs, the cross-linking of free 3-APTES occurs on these surfaces, resulting in the multilayer polysiloxane shells on the MWNTs. In all cases, solvent could be removed in vacuo to collect solid Si-MWNT. No desorption of the siloxane was observed, which was confirmed by TEM imaging and element analysis again. The solid Si-MWNTs could redisperse in distilled water with sonication, which also verified that the polysiloxane shell did not desquamate from the nanotubes surfaces during dry process. The above-mentioned results suggest that the functionalization of MWNTs is stabilized.

In a typical experiment for defunctionalization of Si-MWNTs,<sup>15</sup> a purified sample of Si-MWNT (0.1 mg) was dispersed in 1 mL of distilled water. After 200  $\mu$ L of HF was added, the suspension was ultrasonicated for 2 h, resulting in the formation of dark colored precipitates. The sample obtained was centrifuged and washed repeatedly with chloroform, water, and acetone and then dried. EDX characterization of the samples only shows C and Au peaks for the defunctionalized Si-MWNTs dropped on the gold substrate (Figure S3 of the Supporting Information). It is difficult to detect O, Si, and N peaks because of the removal of polysiloxane from nanotube surfaces by defunctionalization. In addition, the defunctionalized Si-MWNTs can be re-embedded in the polysiloxane shell, which indicates that the route for functionalized MWNTs is a reproducible strategy.

In next experiments, SEM images confirmed that negatively charged gold nanoparticles were successfully self-assembled on Si-MWNT surfaces by electrostatic interactions. The gold nanoparticles are seen as bright spots on the nanotubes surfaces. Figure 4 presents representative SEM micrographs of Si-MWNTs attached with 4–6 nm gold nanoparticles. Most gold nanoparticles distribute almost uniformly on the walls and ends of the nanotubes, although a few aggregates consisting of several nanoparticles are observed (Figure 6A), as are previously demonstrated for self-assemblies of nanoparticles on a planar substrate.<sup>16</sup> The average diameters of the nanoparticles before and after the assembly do not obviously vary. Since the attachment of the gold nanoparticles involves interaction of amino groups and gold nanoparticles, the decoration also serves to confirm our scheme that the amino groups extrude outside, instead of being absorbed on the sidewalls of nanotubes as previous reported.<sup>5g</sup> It is also noted that the interaction between the gold nanoparticles and nanotubes is quite strong, because gold nanoparticles cannot be ripped off the nanotube surfaces through washing.<sup>8c</sup> To further prove that the surfaces of the Si-MWNTs were decorated with positively charged amino groups, we performed similar assembly experiment by using positively charged gold nanoparticles as targets. Briefly, the CTAB-capped





**Figure 3.** Representative TEM images showing (A) a low-magnification micrograph of purified Si-MWNTs and (B) a high-magnification view of purified Si-MWNTs.

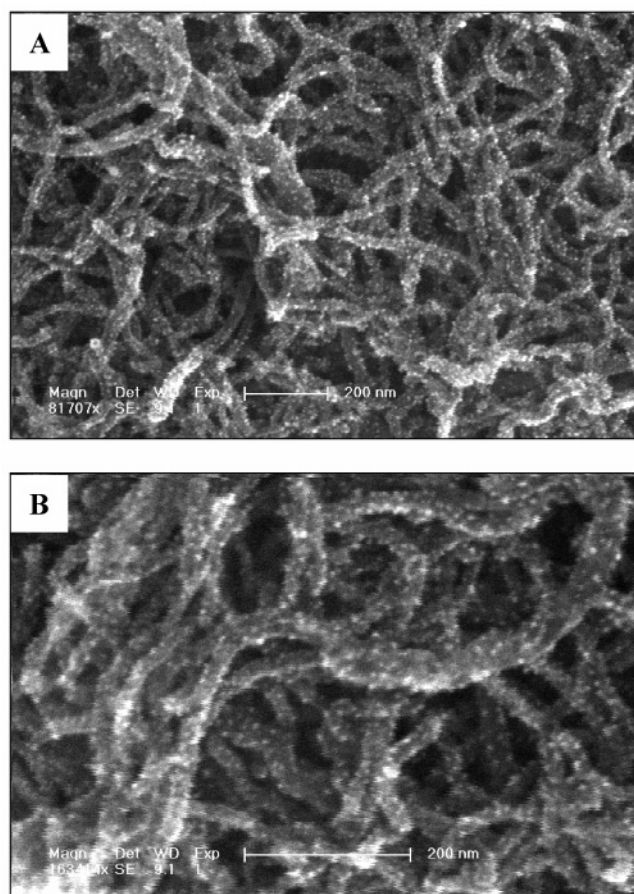


**Figure 4.** SEM images for Si-MWNTs decorated with gold nanoparticles at various magnifications.

4-nm gold nanoparticles were prepared according to our previous report.<sup>17</sup> Subsequently, the positively charged gold nanoparticles were mixed with Si-MWNTs. Nanoparticles did not attach to the surface of the Si-MWNTs. The unsuccessful results demonstrate that the as-prepared Si-MWNTs is indeed positively charged.

The adsorption of nanoparticles was also supported by UV–visible spectra. Figure 5 shows UV–visible absorption spectra of nanoparticles before and after attaching onto Si-MWNT surfaces. For gold nanoparticles, the plasmon band appears at 515 nm, as expected. For Si-MWNTs incubated in this gold colloid for 2 h, even after repeated centrifuging and washing six times, the peak appears at 530 nm, albeit at a decreased

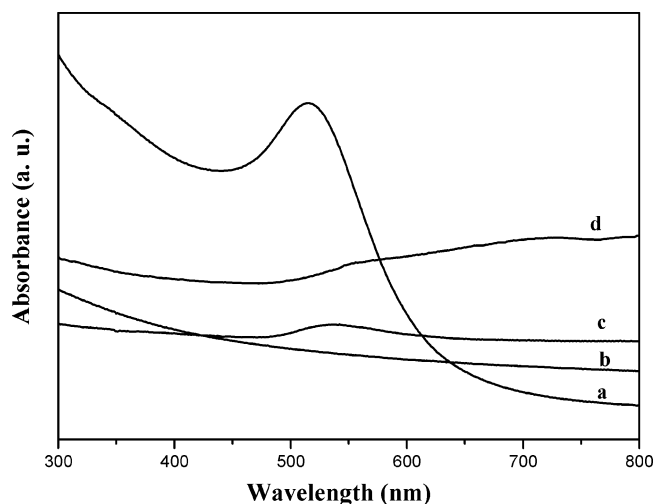


**Figure 5.** UV–visible absorption spectra of gold nanoparticles (a), Si-MWNTs (b), gold nanoparticles attached to the Si-MWNT surfaces (c), and gold wires by growing nanoparticles in distilled water (d), respectively.

intensity. The red-shift of surface-plasmon band can be attributed to the interparticles interactions adsorbed on the Si-MWNTs, as was previously demonstrated by Giersig et al.<sup>9a</sup> This result indicates that the gold nanoparticles are bound to the Si-MWNTs. As a control, the MWNTs without polysiloxane shells were mixed with gold nanoparticles for 2 h, and no peak in UV–visible spectra was observed after washing. This indicates that the gold nanoparticles do not bind to the nanotubes and are removed during repeated washing. Obviously, the polysiloxane shell plays a key role in the attachment, which acts as a bridge to connect gold nanoparticles with nanotubes.

Altering self-assembly time obviously influences the density of negatively charged gold nanoparticles attached on the surfaces of Si-MWNTs. Figure 6 shows typical TEM micrographs corresponding to Si-MWNTs decorated with different coverage of nanoparticles obtained at different assembly times (1 and 8 h, respectively). The assembled nanoparticles display a spatially isolated feature, and the packing density increases with prolonging interactional time. Nanowires cannot be obtained even through longer self-assembly times. This is attributed to the electric double layer repulsion coming from the  $\zeta$ -potential of both similarly charged surfaces.<sup>8b</sup> In addition, Murphy et al. observe that aggregation of citrate-capped gold nanoparticles occurs if aged a long time in mother solution.<sup>13</sup> Therefore, the change in the size of gold nanoparticles adsorbed on the

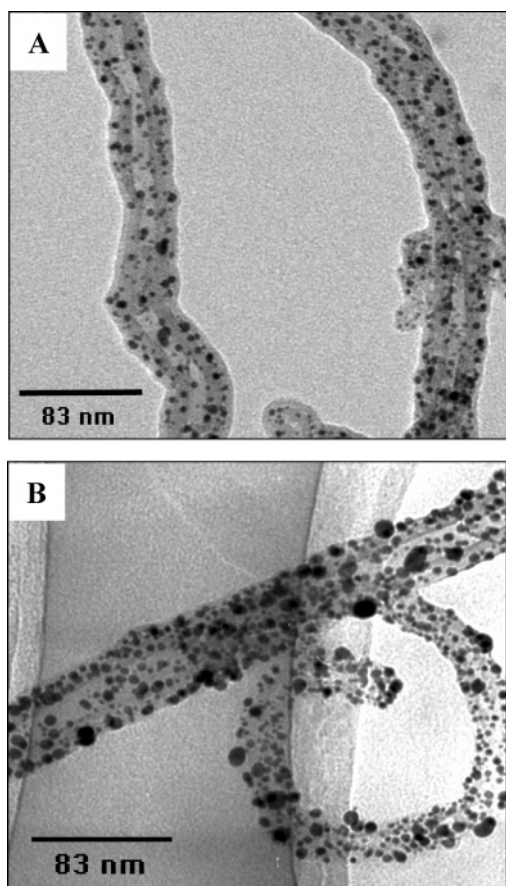


**Figure 6.** TEM micrographs for attachment of gold nanoparticles under different assembly times: (A) 1 h and (B) 8 h.

nanotubes may be attributed to the feeble stabilization of citrate for gold nanoparticles.

To obtain gold nanowires, the Si-MWNTs decorated with gold nanoparticles were dispersed in  $\text{HAuCl}_4$  and then heated at  $100\text{ }^\circ\text{C}$  for 30 min (Figure 7). The TEM image of gold nanoparticles/Si-MWNTs hybrid in  $\text{HAuCl}_4$  aqueous solution before heating is shown in Figure 7A. After heating for 5 min, the shape and size of spherical nanoparticles are changed, indicating that the  $\text{HAuCl}_4$  has been reduced, wherein the initial gold nanoparticles serve as nucleation centers. These nanoparticles are further grown, enlarged, and joined together with neighboring nanoparticles by extending reaction time to 15 min. The joining of discrete gold nanoparticles continues with further prolonging reaction time to 30 min. As a result, the gold nanowires are formed. The gold nanowires follow precisely along the nanotube skeleton. After that, longer heat treatment has less effect on the gold nanowire morphologies. For comparison, if we use the Si-MWNTs without gold nanoparticles on their surfaces as template, the gold nanowires cannot be obtained by directly heating in  $\text{HAuCl}_4$  solution. It is indicated that the presence of gold nanoparticles on the Si-MWNTs is the key for the formation of gold nanowires.

The construction of gold nanowires involves the gold nanoparticles decorated along the Si-MWNTs and the amino groups presented at nanotube surfaces. Amine-containing small molecules, such as hydrazine, can serve as reducing agents for the formation of gold nanoparticles from  $\text{HAuCl}_4$ .<sup>18</sup> Recently, our group presented a heat-treatment-based strategy for the one-step preparation of dendrimer-protected gold nanoparticles with the use of amine-functionalized third-generation poly(propyleneimine) dendrimer (PPI-G3) to simultaneously act both as the reducing agent and protective agent.<sup>19</sup> It is the amino groups

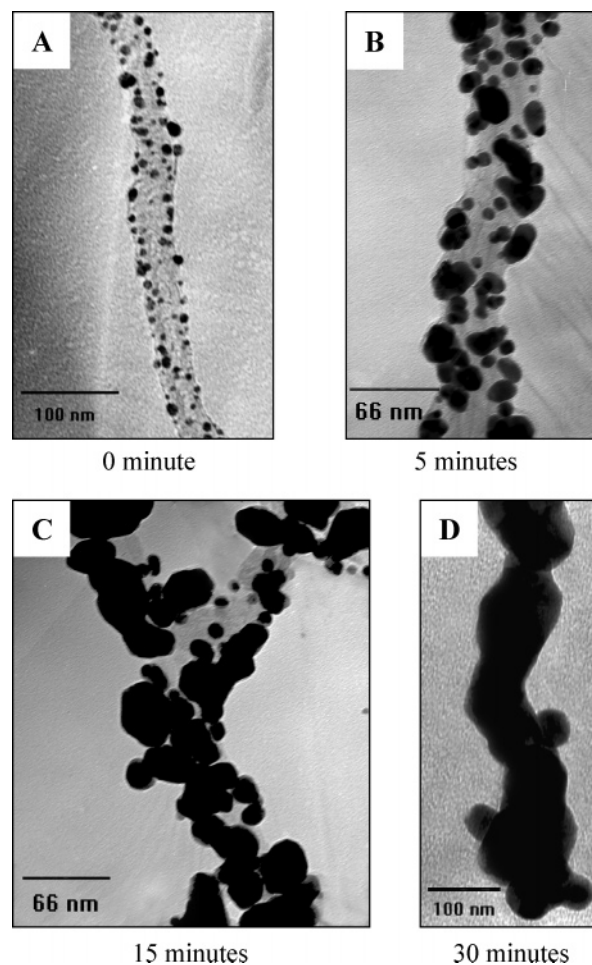


**Figure 7.** TEM images of gold nanoparticles self-assembled on nanotube surfaces prior to and following heating in  $\text{HAuCl}_4$  aqueous solution for the indicated time (A, 0 min; B, 5 min; C, 15 min; D, 30 min).

that reduce  $\text{AuCl}_4^-$  and gradually led to the formation of gold nanoparticles.<sup>20</sup> The Si-MWNTs decorated with gold nanoparticles were dispersed in  $\text{HAuCl}_4$  aqueous solution and heated in an autoclave. The addition of  $\text{HAuCl}_4$  results in the formation of a polysalt between the amino groups of polysiloxane and  $\text{AuCl}_4^-$ , which facilitates electron transfer (ET) from  $\text{Au}^{\text{III}}$  to the amino groups, and also high temperatures can accelerate the ET rate.<sup>18</sup> In our experiments, these nanoparticles serving as nuclei are subsequently further developed by the reduction of  $\text{HAuCl}_4$  along the nanotube surfaces. When the process is continuous, the growing nanoparticles will be joined to form continuous nanowires within several minutes by heating the suspension. Obviously, the self-assembled gold nanoparticles based on Si-MWNTs template give rise to gold nanowires, their length depends on the Si-MWNTs used.

The UV–visible spectrum for gold nanowires with Si-MWNTs serving as template is shown (curve d in Figure 5). The gold nanowires have a weak transverse plasmon band at 550 nm. Generally, for the higher aspect ratio gold nanorods, the short wavelength plasmon band becomes very weak.<sup>21</sup> However, we did not observe a longitudinal plasmon band in the near-IR region. According to the experiments of Murphy et al.,<sup>13,22</sup> as the aspect ratio of gold nanorods increases, the long wavelength plasmon band moves into the near-IR region, even beyond 1800 nm. In addition, we think that the plasmonic frequency of nanowires may be influenced by Si-MWNTs templates.



## Conclusions

We developed a reproducible strategy to noncovalently functionalize carbon nanotubes, resulting in improvement of the MWNTs dispersibility in water. The siloxane is polymerized on the nanotube surfaces and the carbon nanotube is embedded within the polysiloxane shell with a hydrophilic amino group situated outside. The method is effective for the functionalization and dispersibility of carbon nanotubes. Compared to previous techniques for the treatment of carbon nanotubes,<sup>23</sup> the strategy employed in the present study is more simple, mild, and practical. It provides good opportunities to produce more functional groups on surfaces of carbon nanotubes, as is seen to allow deposition of much higher loading of gold nanoparticles without aggregation, in which the presence of nanoparticles identifies the amino groups on the nanotubes extruding outside rather than inside. In addition, the versatility of this method can be extended to join other functionalities, such as biomolecular, semiconducting, and nonconducting nanoparticles of different sizes and shapes, which will result in a range of nanohybrids with different properties. Here, gold nanoparticles are selectively deposited on the surfaces of Si-MWNTs. More interestingly, when the resulting nanoscale structures are heated in HAuCl<sub>4</sub> aqueous solution, the amino group can reduce HAuCl<sub>4</sub> and the gold nanoparticles serving as nuclei are further enlarged, as a result of continuous gold nanowires with carbon nanotubes serving as templates. More works exploring the strategy discussed are under way.

**Acknowledgment.** This work was supported by the National Natural Science Foundation of China (Nos. 20575064 and 20427003).

**Supporting Information Available:** Photographs of MWNTs in distilled water before and after the addition of 3-APTES (Figure S1), a photograph of Si-MWNTs redispersed in distilled water (Figure S2), and EDX diagrams of defunctionalized Si-MWNTs with gold substrates (Figure S3). This material is available free of charge via the Internet at <http://pubs.acs.org>.

## References and Notes

- Benoit, J. M.; Corraze, B.; Chauvet, O. *Phys. Rev. B* **2002**, *65*, 241405.
- Treacy, M.; Ebbesen, T.; Gibson, J. *Nature* **1996**, *381*, 678–680.
- Tans, S.; Devoret, M.; Dai, H.; Thess, A.; Smalley, R.; Geerligs, L.; Dekker, C. *Nature* **1997**, *386*, 474–477.
- Chen, J.; Hamon, M.; Hu, H.; Chen, Y.; Rao, A.; Eklund, P.; Haddon, R. *Science* **1998**, *282*, 95–98.
- (a) Wang, J.; Musameh, M.; Lin, Y. *J. Am. Chem. Soc.* **2003**, *125*, 2408–2409. (b) Hirsch, A. *Angew. Chem. Int. Ed.* **2002**, *41*, 1853–1859. (c) Lordi, V.; Yao, N.; Wei, J. *Chem. Mater.* **2001**, *13*, 733–736. (d) Chen, R.; Zhang, Y.; Wang, D.; Dai, H. *J. Am. Chem. Soc.* **2001**, *123*, 3838–3839. (e) O'Connell, M.; Boul, P.; Ericson, L.; Huffman, C.; Wang, Y.; Haroz, E.; Kuper, C.; Tour, J.; Ausman, K.; Smalley, R. *Chem. Phys. Lett.* **2001**, *342*, 265–271. (f) Star, A.; Stoddart, J.; Steuerman, D.; Diehl, M.; Boukai, A.; Wong, E.; Yang, X.; Chung, S.; Choi, H.; Heath, J. *Angew. Chem., Int. Ed.* **2001**, *40*, 1721–1725. (g) Fu, Q.; Lu, C.; Liu, J. *Nano Lett.* **2003**, *3*, 275–277. (h) Gavalas, V. G.; Law, S. A.; Ball, J. C.; Andrews, R.; Bachasa, L. G. *Anal. Biochem.* **2004**, *329*, 247–252. (i) Luong, J. H. T.; Hrapovic, S.; Wang, D. S.; Bensebaa, F.; Simard, B. *Electroanalysis* **2004**, *16*, 132–139. (j) Gavalas, V. G.; Andrews, R.; Bhattacharyya, D.; Bachasa, L. G. *Nano Lett.* **2001**, *1*, 719–721. (k) Gong, K. P.; Zhang, M. N.; Yan, T. M.; Su, L.; Mao, L. Q.; Xiong, S. X.; Chen, Y. *Anal. Chem.* **2004**, *76*, 6500–6505. (l) Lin, Y.; Rao, A.; Sadanadan, B.; Kenik, E.; Sun, Y. *J. Phys. Chem. B* **2002**, *106*, 1294–1298.
- (a) Daniel, M.; Astruc, D. *Chem. Rev.* **2004**, *104*, 293–346. (b) Rahman, G.; Guldi, D.; Zambon, E.; Pasquato, L.; Tagmatarchis, N.; Prato, M. *Small* **2005**, *1*, 527–530.
- Xing, Y. *J. Phys. Chem. B* **2004**, *108*, 19255–19259.
- (a) Carrillo, A.; Swartz, J.; Gamba, J.; Kane, R. *Nano Lett.* **2003**, *3*, 1437–1440. (b) Kim, B.; Sigmund, W. *Langmuir* **2004**, *20*, 8239–8242. (c) Jiang, K.; Eitan, A.; Schadler, L.; Ajayan, P.; Siegel, R.; Grobert, N.; Mayne, M.; Reyes-Reyes, M.; Terrones, H.; Terrones, M. *Nano Lett.* **2003**, *3*, 275–277. (d) Ellis, A.; Vijayamohan, K.; Goswami, R.; Chakrapani, N.; Ramanathan, L.; Ajayan, P.; Ramanath, G.; *Nano Lett.* **2003**, *3*, 279–282. (e) Han, L.; Wu, W.; Kirk, F.; Luo, J.; Maye, M.; Kariuki, N.; Lin, Y.; Wang, C.; Zhong, C. *Langmuir* **2004**, *20*, 6019–6025.
- (a) Correa-Duarte, M. A.; Sobal, N.; Liz-Marzán, L. M.; Giersig, M. *Adv. Mater.* **2004**, *16*, 2179–2184. (b) Day, T.; Unwin, P.; Wilson, N.; Macpherson, J. *J. Am. Chem. Soc.* **2005**, *127*, 10639–10647. (c) Quinn, B.; Dekker, C.; aLemay, S. *J. Am. Chem. Soc.* **2005**, *127*, 6146–6147. (d) Qu, L.; Dai, L. *J. Am. Chem. Soc.* **2005**, *127*, 10806–10807. (e) Correa-Duarte, M.; Pérez-Juste, J.; Sánchez-Iglesias, A.; Giersig, M.; Liz-Marzán, L. *Angew. Chem., Int. Ed.* **2005**, *44*, 4375–4378. (f) Zanella, R.; Basiuk, E.; Santiago, P.; Basiuk, V.; Mireles, E.; Puente-Lee, I.; Saniger, J. *J. Phys. Chem. B* **2005**, *109*, 16290–16295. (g) Sainsbury, T.; Stolarczyk, J.; Fitzmaurice, D. *J. Phys. Chem. B* **2005**, *109*, 16310–16325.
- (a) Hu, X.; Wang, T.; Qu, X.; Dong, S. *J. Phys. Chem. B* **2006**, *110*, 853–857. (b) Fullam, S.; Cottell, D.; Rensmo, H.; Fitzmaurice, D. *Adv. Mater.* **2000**, *12*, 1430–1432.
- (a) Ongaro, A.; Griffin, F.; Beecher, P.; Nagle, L.; Iacopino, D.; Quinn, A.; Redmond, G.; Fitzmaurice, D.; *Chem. Mater.* **2005**, *17*, 1959–1964. (b) Nagle, L.; Fitzmaurice, D. *Adv. Mater.* **2003**, *15*, 933–935. (c) Korgel, B.; Fitzmaurice, D. *Adv. Mater.* **1998**, *10*, 661–665.
- Zhang, M.; Yudasaka, M.; Iijima, S. *J. Phys. Chem. B* **2005**, *109*, 6037–6039.
- Gao, J.; Bender, C.; Murphy, C. *Langmuir* **2003**, *19*, 9065–9070.
- (a) Kaneko, Y.; Iyi, N.; Kurashima, K.; Matsumoto, T.; Fujita, T.; Kitamura, K. *Chem. Mater.* **2004**, *16*, 3417–3423. (b) Wang, T.; Wang, M.; Hu, X.; Qu, X.; Zhao, F.; Dong, S. *Langmuir* **2005**, *21*, 12068–12071.
- Fu, K.; Huang, W.; Lin, Y.; Riddle, L.; Carroll, D. Sun, Y. *Nano Lett.* **2001**, *1*, 439–441.
- (a) Zheng, J.; Zhou, Y.; Li, X.; Ji, Y.; Lu, T.; Gu, R. *Langmuir* **2003**, *19*, 632–636. (b) Cheng, W.; Dong, S.; Wang, E. *Chem. Mater.* **2003**, *15*, 2495–2501.
- Hu, X.; Cheng, W.; Wang, T.; Wang, Y.; Wang, E.; Dong, S. *J. Phys. Chem. B* **2005**, *109*, 19385–19389.
- He, J.-A.; Valluzzi, R.; Yang, K.; Dolukhanyan, T.; Sung, C.; Kumar, J.; Tripathy, S. *Chem. Mater.* **1999**, *11*, 3268–3274.
- Sun, X.; Jiang, X.; Dong, S.; Wang, E. *Macromol. Rapid Commun.* **2003**, *24*, 1024–1028.
- (a) Sun, X.; Dong, S.; Wang, E. *Polymer* **2004**, *45*, 2181–2184. (b) Won, J.; Ihn, K.; Kang, Y. *Langmuir* **2002**, *18*, 8246–8249. (c) Sun, X.; Dong, S.; Wang, E. *Angew. Chem., Int. Ed.* **2004**, *43*, 6360–6363.
- Obare, S.; Jana, N.; Murphy, C. *Nano Lett.* **2001**, *1*, 601–603.
- Jana, N.; Gearheart, L.; Murphy, C. *J. Phys. Chem. B* **2001**, *105*, 4065–4067.
- (a) Kang, Y.; Taton, T. *J. Am. Chem. Soc.* **2003**, *125*, 5650–5651. (b) Xing, Y.; Li, L.; Chusuei, C.; Hull, R. *Langmuir* **2005**, *21*, 4185–4190.